

A search for lines in the bright X-ray afterglow of GRB 120711A

A. Giuliani¹, S. Mereghetti¹

INAF, Istituto di Astrofisica Spaziale e Fisica Cosmica Milano, via E. Bassini 15, I-20133 Milano, Italy

Received 02/04/2013 / Accepted 16/07/2013

ABSTRACT

GRB 120711A, discovered and rapidly localized by the INTEGRAL satellite, attracted particular interest due to its high γ -ray fluence, very bright X-ray afterglow, and the detection of a prompt optical transient and of long-lasting emission at GeV energies. A follow-up observation carried out with the *XMM-Newton* satellite has provided an X-ray spectrum in the 0.3–10 keV with unprecedented statistics for a GRB afterglow 20 hours after the burst. The spectrum is well fit by a power-law with photon index 1.87 ± 0.01 , modified by absorption in our Galaxy and in the GRB host at $z=1.4$. A Galactic absorption consistent with that estimated from neutral hydrogen observations is obtained only with host metallicity lower than 5% of the Solar value. We report the results of a sensitive search for emission and absorption lines using the matched filter smoothing method (Rutledge & Sako 2003). No statistically significant lines were found. The upper limits on the equivalent width of emission lines, derived through Monte Carlo simulations, are few tens of eV, a factor ~ 10 lower than that of the possible lines reported in the literature for other bursts.

Key words. gamma rays: bursts - methods: data analysis - X-rays: general

1. Introduction

A few detections of X-ray emission and absorption lines in γ -ray bursts (GRB) were reported in the first years after the discovery of GRB afterglows (Piro et al. 2000; Yoshida et al. 2001; Watson et al. 2002; Reeves et al. 2003; Butler et al. 2003; Mereghetti et al. 2003b), based on data obtained with the *BeppoSAX*, *ASCA*, *XMM-Newton*, and *Chandra* satellites. Although the statistical significance of these detections was never higher than 5σ , and more typically around 3σ , these results attracted considerable interest in view of the potential diagnostic for the physics of GRBs and the properties of their environments offered by these putative features (Vietri et al. 2001, and references therein).

After the launch of *Swift*, it has become possible to explore the afterglows at earlier times, but a comprehensive analysis of 40 afterglows observed with the *Swift*/*XRT* instrument failed to detect statistically significant lines (Hurkett et al. 2008). A critical assessment of the possible line features in the nine afterglows reported before 2004 was presented in Sako et al. (2005). These authors performed a uniform, systematic analysis of the spectra obtained with the different instruments and estimated the significance of the lines with Monte Carlo simulations. They also properly took into account the fact that, in the absence of a known redshift, the line energies should be considered as free parameters. This increases the number of independent searches and the detection significances have to be reduced accordingly. In their analysis, Sako et al. (2005) obtained lower significances for these lines, compared to those claimed in the previous papers. Other effects, e.g., the different continuum components adopted in the spectral fit, the estimates of the background, and imperfections in the instrumental response matrices, can also lead to discordant results on the line detections significance. For example, according to Butler et al. (2005), the lines from low- Z elements in GRB 011211 are at the $\sim 3\sigma$ level only if the interstellar

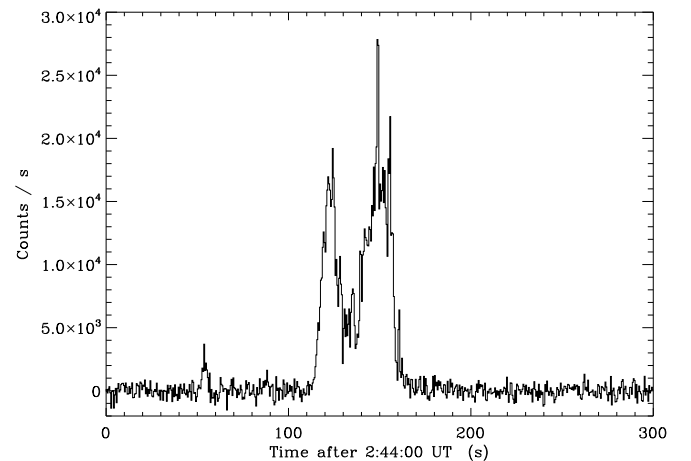


Fig. 1. Light curve of GRB 120711A at $E > 80$ keV in bins of 0.5 s measured with the anti-coincidence system of the SPI instrument.

absorption is fixed at the Galactic value, while their significance decreases if the column density is allowed to vary.

Even if the statistical evaluation is done properly and all the technical issues are carefully taken into account, a great limitation to line searches comes from the small counting statistics of the available spectra. The instrument with the largest collecting area used so far in these studies is the EPIC camera on *XMM-Newton*, but its observations are generally done when the afterglow flux has significantly decreased, since a few hours are needed to re-point this satellite after a GRB discovery.

Here we report on an *XMM-Newton* observation of the very bright GRB 120711A which, providing an afterglow spectrum of unprecedented statistics, offers the possibility to carry out a very sensitive search for spectral features.

Send offprint requests to:

2. GRB 120711A

GRB 120711A was discovered with the IBIS instrument (Ubertini et al. 2003) on the INTEGRAL satellite (Gotz et al. 2012). Its light curve, obtained with the anti-coincidence system (ACS) of the INTEGRAL SPI instrument (von Kienlin et al. 2003), is shown in Fig. 1. The INTEGRAL Burst Alert System (IBAS, Mereghetti et al. (2003a)) triggered on the precursor peak that occurred at about 02:44:50 UT. The rapid IBAS localization allowed the identification of an optical transient (Laclyuze et al. 2012b) reaching a V band magnitude of ~ 12 roughly 112 seconds after the trigger (Laclyuze et al. 2012a), while the hard X-ray prompt emission was still active.

The burst had a fluence of 5×10^5 ACS counts, which corresponds to $\sim 5 \times 10^{-5}$ erg cm $^{-2}$ in the 75 keV - 1 MeV energy range¹. This agrees with the values of a few 10^{-4} erg cm $^{-2}$ ($E > 20$ keV) measured by several other instruments (Hanlon et al. 2012; Golenetskii et al. 2012; Gruber & Pelassa 2012).

GRB 120711A is among the bursts with the highest fluence ever detected (see. e.g. Goldstein et al. 2012; Meegan et al. 1996). Its time integrated spectrum is well described by a Band function with typical parameters of hard GRBs, $\alpha = -1$, $\beta \sim -2.5$, and $E_{peak} \sim 1$ MeV (Gruber & Pelassa 2012; Golenetskii et al. 2012).

Also the X-ray afterglow of GRB 120711A was particularly bright. Immediately after the main burst, significant emission at energy above ~ 15 keV was detected for at least 1000 s in IBIS (Bozzo et al. 2012) and for 800 s in the 20-100 keV range with SPI (Hanlon et al. 2012). *Swift/XRT* started to observe the GRB position 2.3 hours after the prompt emission and detected X-ray emission with a light curve decaying as a power-law with index $1.59^{+0.16}_{-0.15}$ (Beardmore & Evans 2012). The X-ray flux measured 11 hr after the burst was 2.96×10^{-11} erg cm $^{-2}$ s $^{-1}$. Compared to all the other X-ray afterglows observed by *Swift*, this is the third brightest ever, lying at about 3σ from the average in the distribution of the afterglow fluxes measured with *Swift/XRT*.

A suggested photometric redshift of $z \sim 3$ (Elliott et al. 2012) was not confirmed by optical spectroscopic observations, which showed, instead, absorption lines of MgII and FeII at $z=1.405$ (Tanvir et al. 2012). In the following, we will assume this value for the redshift of GRB 120711A.

3. Observations and data reduction

The *XMM-Newton* satellite started to observe the afterglow of GRB 120711A on July 12, 2012 at 00:30 UT. The observation lasted 52 ks. Here we concentrate on the data obtained with the EPIC pn instrument, which consists of a CCD camera operating in the 0.2-12 keV energy range and with an energy resolution (FWHM) of ~ 90 eV at 1.5 keV and ~ 150 eV at 6 keV (Strüder et al. 2001). The instrument was operating in the Full Frame mode, giving a time resolution of 73 ms, and with the thin optical blocking filter.

We processed the EPIC data with version 12 of the *XMM-Newton* Standard Analysis Software (SAS v12). The data were cleaned by discarding a few time intervals of enhanced background, which resulted in a live time exposure of 35.2 ks. For the source spectrum we used mono- and bi-pixel events ($PATTERN \leq 4$) extracted from a circular region with radius of $40''$ and rebinned to have at least 30 counts for each energy channel.

¹ The ACS does not provide spectral information; we adopted the average conversion factor derived by Viganò & Mereghetti (2009).

The background spectrum was extracted from a source-free region on the same chip as the target. Spectral fits were done with the XSPEC 12.7.0 package. For the Galactic interstellar absorption we used the *phabs* model, with abundances from Anders & Grevesse (1989).

4. Spectral analysis

We fit the EPIC/pn spectrum in the 0.3-10 keV energy range with a power law model modified by interstellar absorption in our Galaxy, N_H^{Gal} , and in the GRB host, $N_H^{Host}(z)$, with redshift fixed at $z=1.405$. The best fit obtained using Solar abundances in the host absorption resulted in a low N_H^{Gal} , inconsistent with the value of 7.8×10^{20} cm $^{-2}$ estimated from HI observations in this direction (Kalberla et al. 2005). Allowing the metallicity in the host absorption to vary, resulted in metals abundances $\lesssim 10\%$ Solar and $N_H^{Gal} = (8.5^{+0.8}_{-1.6}) \times 10^{20}$ cm $^{-2}$, fully consistent with the Galactic value. We therefore fixed $N_H^{Gal} = 7.8 \times 10^{20}$ cm $^{-2}$ and obtained the following best fit parameters: power-law photon index $\Gamma = 1.87 \pm 0.01$, unabsorbed 0.3-10 keV flux $F = (8.7 \pm 0.1) \times 10^{-12}$ erg cm $^{-2}$ s $^{-1}$, $N_H^{Host} = (5.1^{+0.5}_{-0.7}) \times 10^{22}$ cm $^{-2}$, and metallicity < 0.05 Solar (reduced $\chi^2 = 1.13$ for 154 d.o.f.).

Hurkett et al. (2008) compared different approaches commonly used to search for lines in X-ray spectra. They showed that the highest sensitivity is obtained with the analysis based on Bayesian posterior predictive probabilities (Protassov et al. 2002) or with the matched filter smoothing method (Rutledge & Sako 2003). In our analysis of the afterglow spectrum of GRB 120711A, we implemented the matched filter smoothing algorithm as follows.

The background-subtracted counts spectrum was convolved with a Gaussian with energy-dependent width $\sigma(E)$. To properly take into account the instrument energy resolution at the time of our observation, we derived $\sigma(E)$ by fitting the response matrix produced with the SAS task RMFGEN. The resulting values of $\sigma(E)$ are well approximated by the relation $\sigma(E) = a + bE + cE^2$, with $a=0.0422$, $b=0.0100$, $c=-0.000535$ and the energy E in keV. These values differ from those used in Rutledge & Sako (2003) due to the degradation of the CCD performances with time, which resulted in a $\sim 20\%$ worse energy resolution. The Gaussian-convolved spectrum is shown in Fig. 2.

To establish the threshold values to use in the line search we simulated 10^5 spectra with the best fit continuum model described above and convolved them in the same way used for the GRB 120711A data. The distributions of the resulting number of counts in each energy channel were then used to derive the percentile curves shown by the dashed lines in Fig. 2, which correspond to single trial detection significances of 2, 3 and 4 σ . The convolved data and threshold levels, divided by the model for a better visualization, are shown in the bottom panel of the figure.

The largest deviations in the observed spectrum, occurring at ~ 6.80 and ~ 8.23 keV, reach only the 3 σ confidence level. Given that there is no a-priori reason to expect a line at any of these energies, we have to consider the number of independent trials, which can be taken as the number of resolution elements in the explored energy range, ~ 120 , which makes the detection not significant. We repeated the analysis using the model with parameters fixed at the values corresponding to their 2σ error regions. Also in this case no significant features were found. We therefore conclude that there is no evidence for emission or absorption lines in the EPIC/pn spectrum of the GRB 120711A afterglow.

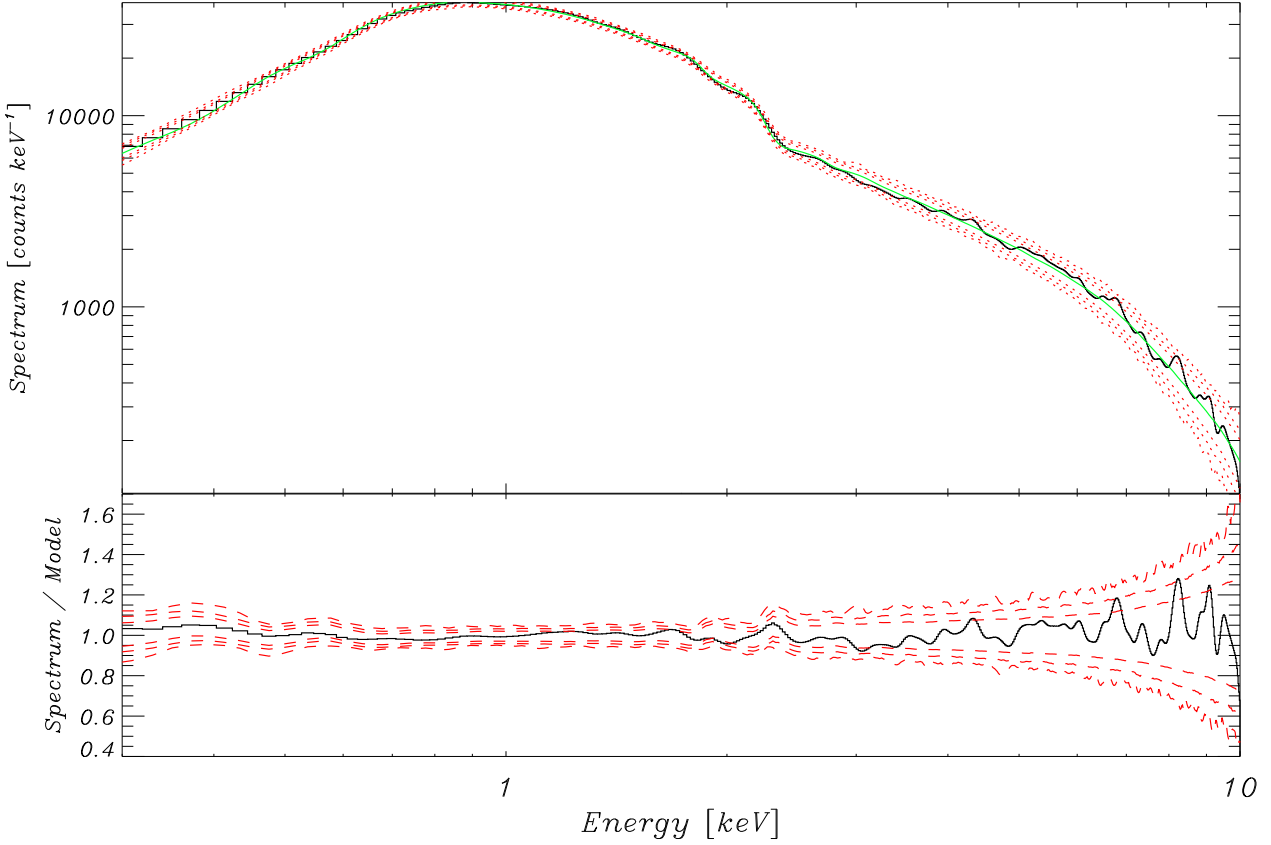


Fig. 2. Upper panel: Spectrum of the X-ray afterglow of GRB 120711A convolved with a Gaussian as described in the text (black solid line). The best-fit model is shown by the green line. The dashed lines are the percentile curves obtained with the simulations for emission and absorption lines. They correspond to single-trial detection significance of 2, 3 and 4σ . Lower panel: the same curves of the upper panel, normalised by dividing by the best-fit model.

To estimate the upper limits on emission lines we simulated spectra of GRB 120711A with Gaussian lines of different widths ΔE , centroid energy, and intensity added to the continuum model. In this way we determined the line intensities that would exceed our 4σ threshold in more than 90% of the cases. These intensities are plotted in Fig. 3 for the cases of $\Delta E=0$ (i.e. non-resolved lines) and $\Delta E=200$ eV and the best fit model with $z=1.405$. The value of $\Delta E=200$ eV has been chosen as representative for the lines previously reported in the literature (see Sako et al. 2005). As done for the emission lines, the limits for the lines in absorption were computed assuming Gaussian profiles, with widths of 0 eV and 200 eV. These limits are shown in Fig. 4 in terms of optical depth at line center.

Two further *XMM-Newton* observations of GRB 120711A were performed on 2012 July 28-29 and August 15. Although they provide a lower sensitivity compared to the first observation, due to the source fainter flux and shorter exposure time, we analysed also these data to search for emission lines, possibly appearing at a late time. None was found, with equivalent width upper limits about one order of magnitude higher than those of Fig. 3.

5. Discussion and conclusions

Thanks to the large number of counts collected in the afterglow spectrum of GRB 120711A with the *XMM-Newton* EPIC instrument we have performed a search for emission and absorption lines with unprecedented sensitivity. The EPIC/pn spectrum we

analyzed contained ~ 50000 net counts. For comparison, the afterglow spectrum with the highest statistics previously available was GRB 040106 ($\sim 23,000$ net counts in the EPIC pn plus MOS cameras, Sako et al. 2005). A few features were found in its spectrum, of which the brightest was an emission line at ~ 0.66 keV with equivalent width $EW=39$ eV. However these authors estimated that the significance of these lines was too small to claim a detection.

The equivalent widths of some of the lines reported in the literature for other GRBs are plotted in Fig. 3 for comparison with our upper limits. We only considered the bursts for which lines were claimed with statistical significance greater than 2σ , and plotted in the figure the measured equivalent width in the rest-frame of the bursts. For GRB 970508 (Piro et al. 1999), GRB 970828 (Yoshida et al. 2001), GRB 991216 (Piro et al. 2000), GRB 000214 (Antonelli et al. 2000), and GRB 030227 (Mereghetti et al. 2003b) the reported lines were attributed to highly ionized iron, while lines from H- or He-like ions from lighter elements (Mg to Ca) were claimed in GRB 001025 (Watson et al. 2002), GRB 011211 (Reeves et al. 2003), GRB 020813 (Butler et al. 2003), and GRB 030227 (Watson et al. 2003). A possible line in GRB 010220 was attributed to Ni (Watson et al. 2002).

The equivalent widths reported for these lines are all well above our upper limits, and would hence be largely visible in the afterglow spectrum of GRB 120711A. Our results hence indicate that similar lines are, at least, not common in the spectra of GRBs afterglows.

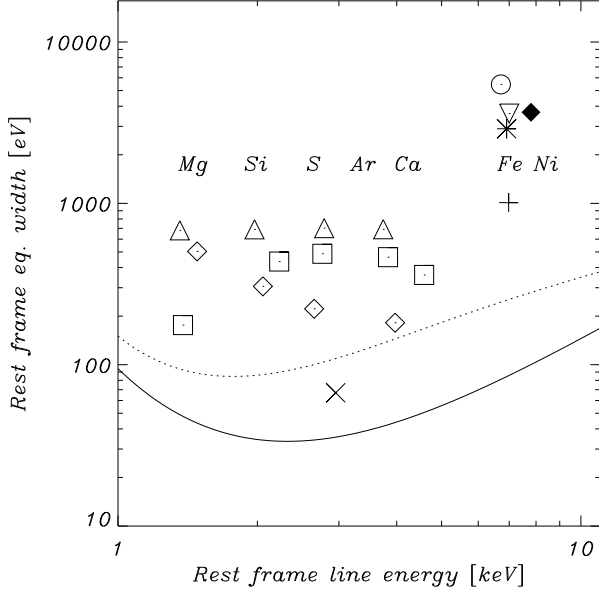


Fig. 3. Upper limits on the equivalent width of emission lines in the afterglow of GRB 120711A in the case of narrow ($\Delta E=0$ eV, solid curve) or wide ($\Delta E=200$ eV, dotted curve) lines. The curves give the best fit (with a 4th-order logarithmic polynomial) to the values obtained from simulations. For comparison, also the rest-frame equivalent widths reported for other GRBs are plotted: \circ GRB 970828, ∇ GRB 970508, $+$ GRB 991216, $*$ GRB 000214, \triangle GRB 001025, squares GRB 010220, filled diamond GRB 011211, \times GRB 020813, \diamond GRB 030227. The energies corresponding to the transition $n=2 \rightarrow 1$ for some H-like ions are also indicated.

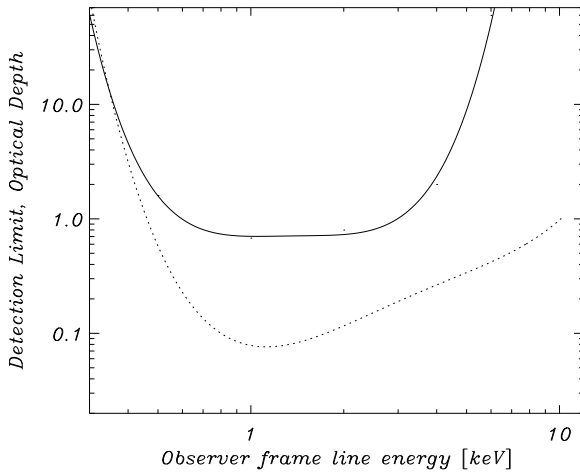


Fig. 4. Upper limits on the optical depth at line center of absorption lines in the afterglow of GRB 120711A in the case of narrow ($\Delta E=0$ eV, solid curve) or wide ($\Delta E=200$ eV, dotted curve) lines. The curves give the best fit (with a 4th-order logarithmic polynomial) to the values obtained from simulations.

We also found evidence for a low-metallicity absorbing medium in the GRB host galaxy. This result supports the suggestion that the high absorption in X-ray afterglows might be mainly due to helium in the HII regions in which the GRBs were born (Watson et al. 2013).

Acknowledgements. This research is based on data of XMM-Newton, an ESA science mission with instruments and contributions directly funded by ESA

Member States and NASA. We thank N.Schartel and the staff at the XMM-Newton Science Operation Center for making this target of opportunity observation and A.Tiengo for advice on the data analysis. This work was partially supported by the ASI/INAF agreement I/033/10/0.

References

- Anders, E. & Grevesse, N. 1989, *Geochim. Cosmochim. Acta*, 53, 197
Antonelli, L. A., Piro, L., Vietri, M., et al. 2000, *ApJ*, 545, L39
Beardmore, A. P. & Evans, P. A. 2012, *GRB Coordinates Network*, 13442, 1
Bozzo, E., Gotz, D., Mereghetti, S., et al. 2012, *GRB Coordinates Network*, 13435, 1
Butler, N., Ricker, G., Vanderspek, R., et al. 2005, *ApJ*, 627, L9
Butler, N. R., Marshall, H. L., Ricker, G. R., et al. 2003, *ApJ*, 597, 1010
Elliott, J., Klose, S., & Greiner, J. 2012, *GRB Coordinates Network*, 13438, 1
Goldstein, A., Burgess, J. M., Preece, R. D., et al. 2012, *ApJS*, 199, 19
Golenetskii, S., Aptekar, R., Frederiks, D., et al. 2012, *GRB Coordinates Network*, 13446, 1
Gotz, D., Mereghetti, S., Bozzo, E., et al. 2012, *GRB Coordinates Network*, 13434, 1
Gruber, D. & Pelassa, V. 2012, *GRB Coordinates Network*, 13437, 1
Hanlon, L., Martin-Carrillo, A., Zhang, X.-L., & von Kienlin, A. 2012, *GRB Coordinates Network*, 13468, 1
Hurkett, C. P., Vaughan, S., Osborne, J. P., et al. 2008, *ApJ*, 679, 587
Kalberla, P. M. W., Burton, W. B., Hartmann, D., et al. 2005, *A&A*, 440, 775
Laluyze, A., Haislip, J., Ivarsen, K., et al. 2012a, *GRB Coordinates Network*, 13433, 1
—. 2012b, *GRB Coordinates Network*, 13430, 1
Meegan, C. A., Pendleton, G. N., Briggs, M. S., et al. 1996, *ApJS*, 106, 65
Mereghetti, S., Götz, D., Borkowski, J., Walter, R., & Pedersen, H. 2003a, *A&A*, 411, L291
Mereghetti, S., Götz, D., Tiengo, A., et al. 2003b, *ApJ*, 590, L73
Piro, L., Costa, E., Feroci, M., et al. 1999, *ApJ*, 514, L73
Piro, L., Garmire, G., Garcia, M., et al. 2000, *Science*, 290, 955
Protassov, R., van Dyk, D. A., Connors, A., Kashyap, V. L., & Siemiginowska, A. 2002, *ApJ*, 571, 545
Reeves, J. N., Watson, D., Osborne, J. P., Pounds, K. A., & O'Brien, P. T. 2003, *A&A*, 403, 463
Rutledge, R. E. & Sako, M. 2003, *MNRAS*, 339, 600
Sako, M., Harrison, F. A., & Rutledge, R. E. 2005, *ApJ*, 623, 973
Strüder, L., Briel, U., & Dennerl, K. e. 2001, *A&A*, 365, L18
Tanvir, N. R., Wiersema, K., Levan, A. J., et al. 2012, *GRB Coordinates Network*, 13441, 1
Ubertini, P., Lebrun, F., Di Cocco, G., et al. 2003, *A&A*, 411, L131
Vietri, M., Ghisellini, G., Lazzati, D., Fiore, F., & Stella, L. 2001, *ApJ*, 550, L43
Viganò, D. & Mereghetti, S. 2009, *ArXiv e-prints*
von Kienlin, A., Beckmann, V., Rau, A., et al. 2003, *A&A*, 411, L299
Watson, D., Reeves, J. N., Hjorth, J., Jakobsson, P., & Pedersen, K. 2003, *ApJ*, 595, L29
Watson, D., Reeves, J. N., Osborne, J., et al. 2002, *A&A*, 393, L1
Watson, D., Zafar, T., Andersen, A. C., et al. 2013, *ApJ*, 768, 23
Yoshida, A., Namiki, M., Yonetoku, D., et al. 2001, *ApJ*, 557, L27